

# Calibration and Performance of the K<sub>a</sub>-band Radar during REFRACCTT 2006

Gordon Farquharson, Jonathan Emmett, and Scott Ellis

November 7, 2006

## 1 Introduction

The K<sub>a</sub>-band radar was deployed during REFRACCTT 2006 to provide dual-wavelength polarimetric capability to S-Pol. The primary reason for participation in the project was to make water vapor retrievals over the refractivity domain of the REFRACCTT project. This document describes the installation, calibration, and performance of the K<sub>a</sub>-band radar during the project.

## 2 Installation

The K<sub>a</sub>-band radar installation started on July 13, 2006, and was completed on July 14, 2006. Networking and RDA setup were performed on July 15, and S-Pol synchronization and a full system test were completed on July 16. The procedure used to test the synchronization with S-Pol, and the dish alignment are outlined below.

### 2.1 Synchronization with S-Pol

To ensure that the S- and K<sub>a</sub>-band radars have matched resolution volumes, radar beams must be formed from data recorded at times common to both radars. To test this, signals are injected into both the S- and K<sub>a</sub>-band receivers every 10 beams. If the systems are using the same hits to form beams, a pattern of spokes will appear on both displays. The circuit used to switch in the signals is shown in Figure 1.

### 2.2 Dish Alignment

The S- and K<sub>a</sub>-band dishes are aligned primarily using solar scans. The process is to collect a solar box scan with the transmitter disabled. The volume consists of numerous PPI scans covering the sun in elevation angle increments of 0.2 degrees. Each ray in the volume are then averaged in range and interpolated onto a Cartesian grid with the x-axis being azimuth angle and the y-axis being elevation angle.

The distortion of the plot due to both the translation of the sun during the volume collection and the lack of proper mathematical coordinate transformation from polar space to a Cartesian grid are not

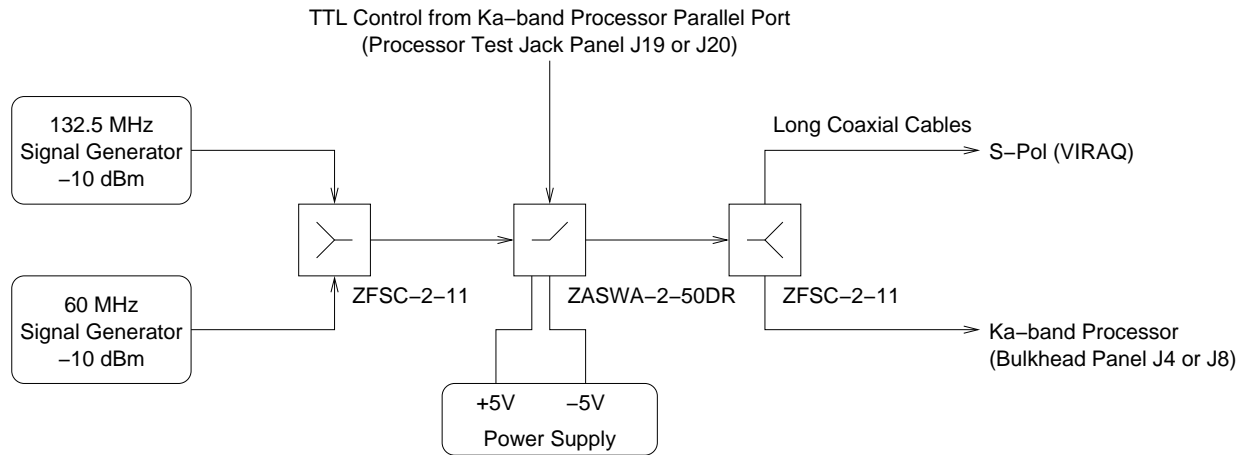


Figure 1: S- and  $K_a$ -band beam alignment test circuit. Signals are injected into both the S- and  $K_a$ -band receivers to check that beams are formed at the same time.

important for dish alignment purposes and are ignored. After overlaying the solar contours of both frequencies, the alignment offsets are determined and the  $K_a$ -band dish alignment adjusted accordingly. This is repeated until the solar patterns are aligned. Figure 2 shows the result of a solar plot after the dishes have been aligned, with the  $K_a$ -band plotted with solid red contours and the S-band plotted with dashed black lines. The variations in the  $K_a$ -band pattern are due to the low signal to noise ratio of the solar measurements. Once the solar alignment is completed the azimuthal alignment is checked using towers of known location.

## 3 Calibration

### 3.1 Receiver Gain

The receiver gain is measured using by injecting a signal into the receiver antenna ports and adjusting the configured gain of the channel such that the power recorded by the system matches the input power. The frequency of the signal was 34.769 GHz which was the nominal frequency of the magnetron when measured in the laboratory.

The H- and V-channel gains were measured to be 44.96 and 44.06 dB respectively. These gains are used to convert the ADC measured voltages to powers which are then converted to reflectivity by applying the radar constant. The power values ( $P$  in ABP) in the archive files should have been derived using these gains.

Measurements from solar scans were used to ensure that the receiver gains set for the H- and V-channels were consistent, i.e. that the powers derived from the ADC voltages matched one another. The maximum value of the power recorded by the system during two solar scans are listed in Table 1. The H-channel power is approximately 0.5 dB less than the V-channels on both days, and the change in power from the first to the second day is consistent in both the H-channel and the V-channel.

The gains of the channels changed when the TR limiters and LNAs were replaced on August 3, 2006 (V-channel) and August 8, 2006 (H-channel). Calibration measurements were not performed when these changes were made, and unfortunately, the LNAs were destroyed which make future calibration measurements impossible.

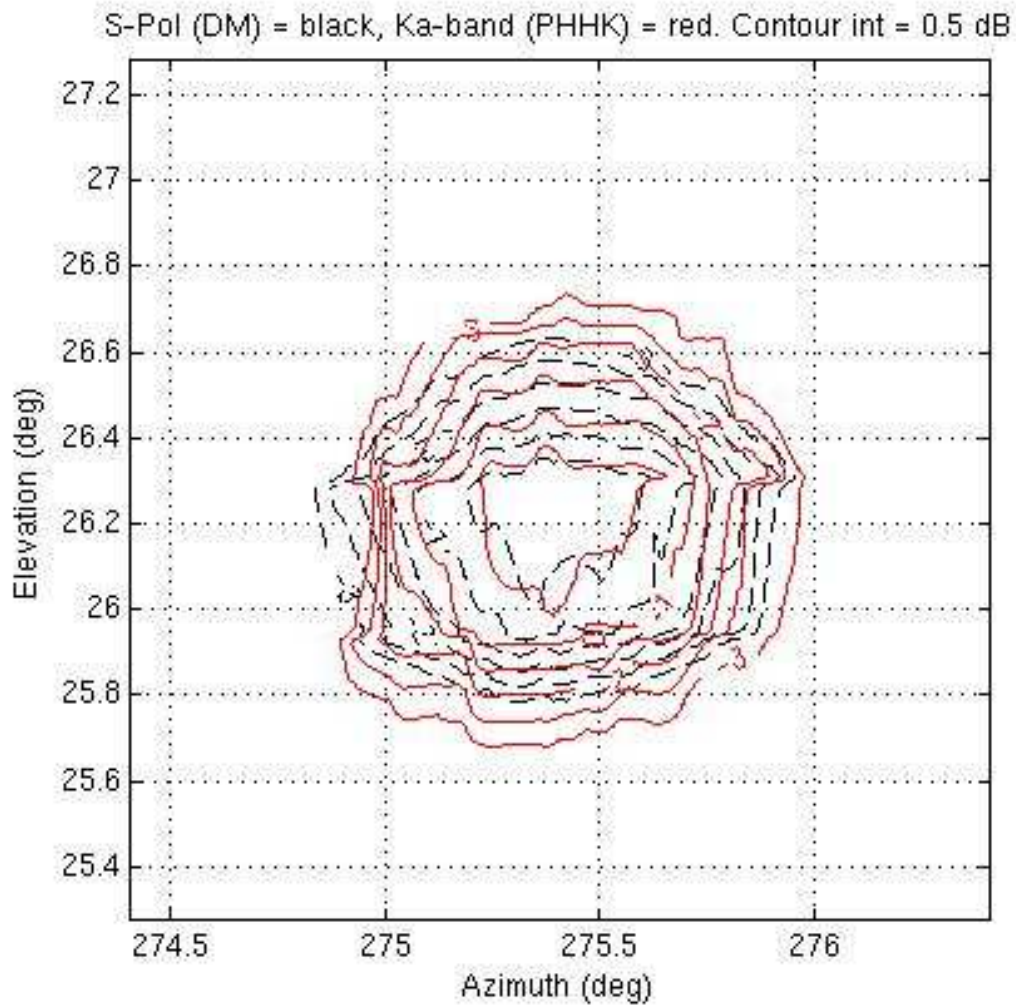


Figure 2: Antenna pattern measurements for S- (black) and K<sub>a</sub>-band (red) radars.

Table 1: Maximum power recorded during solar scan (dBm)

Date	DM	DL	P_HH_K	P_VV_K
2006/07/18	-102.62	-103.11	-105.15	-105.75
2006/07/19	-102.32	-102.85	-105.51	-106.06

## 3.2 Receiver Noise Power

The noise figure of the receiver is measured using the Y-factor method [1].  $50\ \Omega$  waveguide terminations at room temperature are used as the cold load, and a noise source is used for the hot load.

The noise figures measured for the H- and V-channel were 7.0 and 7.8 dB respectively. These translate to system noise powers of around  $-106.5$  and  $-105.7$  dBm respectively for a sky brightness temperature of 120 K. This is the brightness temperature that corresponds to an elevation angle of 5 degrees at 35 GHz [2]. These noise powers are larger than the noise power observed with the radar during REFRACTT. A receiver noise figure of around 5.1 dB is consistent with the measurements and also theoretical calculations of the system noise figure based on specified component values. Thus, there is likely a problem with our implementation of the Y-factor method. This problem will be investigated in the future.

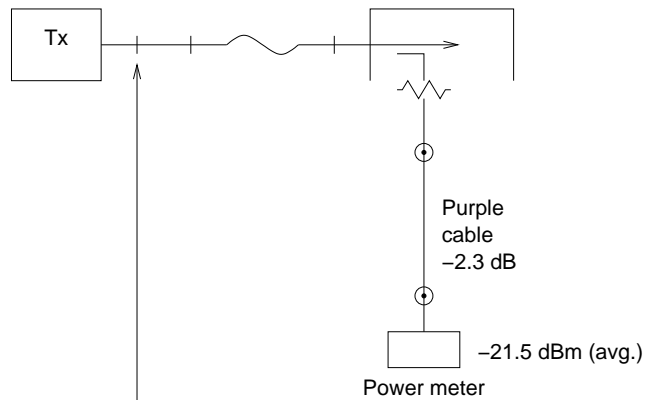
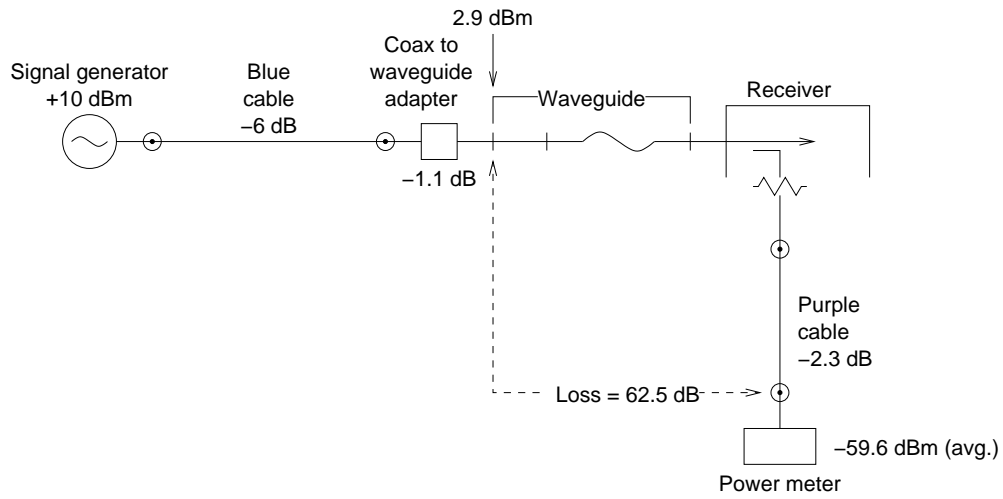
## 3.3 Transmitted Power

The power at the output of the transmitter cabinet was measured in the laboratory using the measurement setup shown in Figure 3. The power meter was attached to the output of the G0 directional coupler in the receiver enclosure as shown in the upper part of Figure 3. The loss between the output of the transmitter cabinet and the power meter was measured by injecting a signal into the waveguide that attaches to the output of the transmitter cabinet, and was found to be 62.5 dB. Then the transmitter was connected to the waveguide (lower part of Figure 3, and the power measured was  $-21.5$  dBm. Thus, the power at the output of the transmitter cabinet was calculated to be  $-21.5 + 62.5 = 41$  dBm. Because the power meter only measures average power, the duty cycle is used to calculate the peak transmitted power. The pulse repetition rate is 480 Hz and the transmitted pulse length of  $0.5\ \mu\text{s}$  which gives a duty cycle of 0.024% ( $-36.2$  dB). Therefore, the peak transmitted power is  $41 - (-36.2) = 77.2$  dBm (52.48 kW). This value is consistent with the measurements made by the transmitter manufacturer.

The waveguide losses between the transmitter and receiver cabinets (including the Tallguide) had been previously measured to be 2.5 dB (Frank Pratte). The loss between the input to the receiver cabinet and the antenna port was measured using the measurement setup shown in Figure 4. A signal is injected into the transmitter port of the receiver cabinet and measured at the input to the antenna. The loss from the transmitter port to the H-channel antenna port was found to be 4.1 dB, and 4.2 dB for the V-channel port. The H-channel transmitted power is therefore  $77.2 - 2.5 - 4.1 = 70.6$  dBm (11.48 kW), and  $77.2 - 2.5 - 4.2 = 70.5$  dBm (11.22 kW) for the V-channel.

## 3.4 Gate 0 (G0) Channel

A fraction of the transmitted power is coupled into the G0 channel for tracking the transmitted frequency and to measure the phase of the transmitted pulse. The gain of this channel is measured in the lab to calibrate the G0 channel. The measurement setup is shown in Figure 5. The measurement of the G0 channel gain is divided into two parts. The first part measures the G0 channel coupling factor. This was found to be  $-48.5$  dB. The second part measures the gain of the rest of the G0 channel from the output of the G0 coupler to the input to the G0 channel of the Sampler card. The gain for this section was  $-29$  dB, and thus the total gain through the G0 channel is  $-77.5$  dB. Thus, the power at the input to the Sampler card G0 channel should be  $-2.8$  dBm for a transmit power of 77.2 dBm at the output of the transmitter cabinet.



$$\text{Tx power} = -21.5 + 62.5 = 41 \text{ dBm (avg.)}$$

$$\text{Peak power} = 41 - (-36.2) = 77.2 \text{ dBm (480 Hz, 0.5 us)}$$

Figure 3: Measurement setup for the transmitted power at the output of the transmitter cabinet.

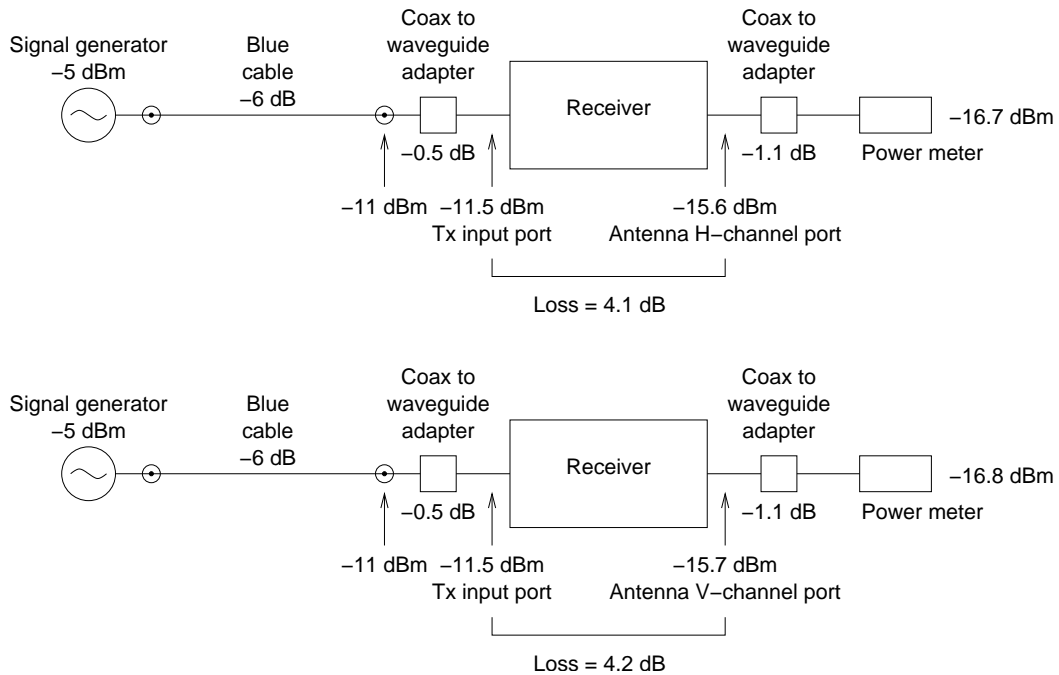


Figure 4: Measurement of the loss between the transmitter input to the receiver cabinet and the antenna port. The upper and lower figures show the measurement of the H- and V-channels respectively.

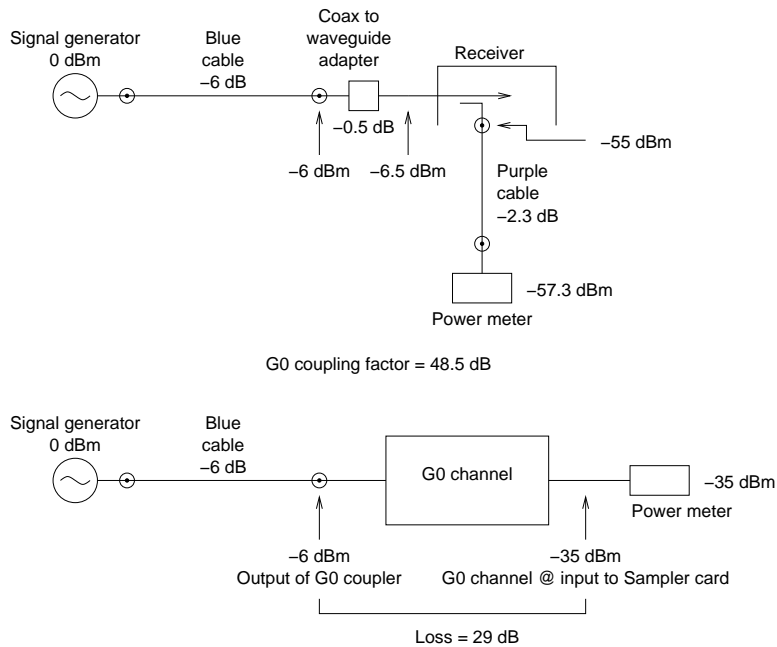


Figure 5: G0 channel calibration setup. The measurement of the G0 channel gain is divided into two measurements. The upper part of the figure shows the measurement of the G0 channel coupler, and the lower part of the figure shows the measurement through the rest of the G0 channel after the coupler.

## 3.5 Radar Constant

The radar constant is used to calculate the reflectivity factor through

$$Z_e = (\text{RC}) r_0^2 l^2 \frac{P(\vec{r}_0)}{g_s} \quad (1)$$

where  $r_0$  is the range to the resolution volume and is in kilometers,  $l$  is the atmospheric attenuation in decibels per kilometer,  $P(\vec{r}_0)$  is the power in milliwatts measured by the analog to digital converter in the system,  $g_s$  is the gain of the receiver (from the antenna to the analog to digital converter, and  $Z_e$  is the reflectivity factor in  $\text{mm}^6/\text{m}^3$ . All of these values are specified or were measured in the laboratory for the  $K_a$ -band system prior to REFRACTT, and are listed in the attached spreadsheet.

The radar constant is calculated from

$$\text{RC} = \frac{2^{10} \ln(2) \lambda^2 l_r}{\pi^3 P_t g^2 \theta_b^2 c \tau |K_w|^2} \times 10^{21} \quad (2)$$

where  $\lambda$  is the electromagnetic wavelength in meters,  $l_r$  is the finite bandwidth power loss,  $P_t$  is the peak transmitted power in watts,  $g$  is the antenna gain,  $\theta_b$  is the beam width of the antenna in radians,  $c$  is the speed of light in meters per second,  $\tau$  is the transmitted pulse length in seconds, and  $|K_w|^2 = 0.93$ .

The value for  $l_r$  depends on the shape of the transmitted pulse and the receiver filter. The  $K_a$ -band system logs two parameters (`hxmit_power_g0` and `hxmit_power_sampler_peak`) in the  $K_a$ -band engineering log file. `hxmit_power_g0` is the average power contained in the transmitted pulse after passing through the receive filter, and `hxmit_power_sampler_peak` is the peak transmitted power sample in the transmitted pulse. For an infinite bandwidth receiver, these would be equal, and there would be no loss due to the filter. The ratio of these is the finite bandwidth power loss ( $l_r$ ) which is used in the radar constant.

The average value of  $l_r$  is listed in Table 2 for  $K_a$ -band periods of operation during REFRACTT (this list is not a comprehensive list of the periods of operation). From July 18 to July 30, the average value of the loss was 7.6 dB and varied within four tenths of a decibel. From July 31 to August 3, the receiver had trouble tracking the frequency of the transmitted pulse, and the average value of the loss increased to between 8.78 to 9.24 dB. The reason was found to be that the transmitted pulse shifted relative to the timing of the radar, and therefore was not being sampled correctly. At the start of the project, the delay from the transmit trigger to the transmitted pulse was 550 ns. This was measured again on August 5 and was found to be 660 ns. When the delay to the transmitted pulse was increased in the processor configuration file by 100 ns, the system was able to track the transmitted frequency again, and  $l_r$  returned to around 7.6 dB (August 6 and 7). No reason has been found for the change in timing of the transmitted pulse.

From this data, the average finite bandwidth power loss is 7.6 dB and the radar constant for the  $K_a$ -band radar during REFRACTT is 73.4 dB. Based on this radar constant, and the noise power calculated for the system, the system sensitivity at various ranges is listed in Tables 3 and 4.

## 4 Data Quality

### 4.1 Expected Reflectivity Accuracy

The theoretical reflectivity accuracy is based on the number of independent samples recorded in a dwell and the signal to noise ratio of the measurement. The number of independent samples is in turn based

Table 2: Finite Bandwidth Power Loss

Start Time	End Time	Loss ( $l_r$ )
Mon Jul 17 21:00:00 2006	Tue Jul 18 00:00:00 2006	6.87
Tue Jul 18 18:00:00 2006	Wed Jul 19 00:00:00 2006	7.35
Wed Jul 19		
Thu Jul 20 17:00:00 2006	Thu Jul 20 22:00:00 2006	7.71
Fri Jul 21 16:00:00 2006	Fri Jul 21 21:00:00 2006	7.67
Sat Jul 22 17:00:00 2006	Sat Jul 22 22:00:00 2006	7.93
Sun Jul 23 18:00:00 2006	Mon Jul 24 00:00:00 2006	7.55
Mon Jul 24		
Tue Jul 25		
Wed Jul 26 19:00:00 2006	Thu Jul 27 00:00:00 2006	7.53
Thu Jul 27 16:00:00 2006	Thu Jul 27 23:00:00 2006	7.64
Fri Jul 28 18:00:00 2006	Sat Jul 29 00:00:00 2006	7.68
Sat Jul 29 20:00:00 2006	Sun Jul 30 00:00:00 2006	7.77
Sun Jul 30 16:00:00 2006	Sun Jul 30 17:00:00 2006	7.56
Mon Jul 31 17:00:00 2006	Tue Aug 1 00:00:00 2006	8.93
Tue Aug 1 02:00:00 2006	Tue Aug 1 14:00:00 2006	9.24
Tue Aug 1 22:00:00 2006	Wed Aug 2 01:00:00 2006	8.97
Wed Aug 2 17:00:00 2006	Thu Aug 3 01:00:00 2006	8.78
Thu Aug 3 17:00:00 2006	Thu Aug 3 23:00:00 2006	8.93
Fri Aug 4		
Sat Aug 5		
Sun Aug 6 17:00:00 2006	Mon Aug 7 00:00:00 2006	7.57
Mon Aug 7 16:00:00 2006	Tue Aug 8 00:00:00 2006	7.38

Table 3: System sensitivity - single pulse

Range (km)	1	3	10	30	50
$Z_{\min}$ 0 dB/km	-34.1	-24.5	-14.1	-4.5	-0.1
$Z_{\min}$ 0.10 dB/km	-33.9	-23.9	-12.1	1.5	9.9

Table 4: System sensitivity - integration over dwell time

Range (km)	1	3	10	30	50
$Z_{\min}$ 0 dB/km	-39.7	-30.2	-19.7	-10.2	-5.8
$Z_{\min}$ 0.10 dB/km	-39.5	-29.6	-17.7	-4.2	4.2

on the spectral width of the scatterers. Table 5 shows the standard deviation of reflectivity for various signal to noise ratio and spectral width values.

Table 5: Standard deviation in reflectivity measurement (dB)

SNR (dB)	Spectral Width ( $\text{m s}^{-1}$ )				
	0.25	0.5	1	1.5	2
0	1.92	1.71	1.67	1.67	1.67
10	1.31	0.99	0.92	0.92	0.92
20	1.26	0.92	0.84	0.84	0.84
30	1.26	0.91	0.84	0.84	0.84

## 4.2 Ghost Echoes

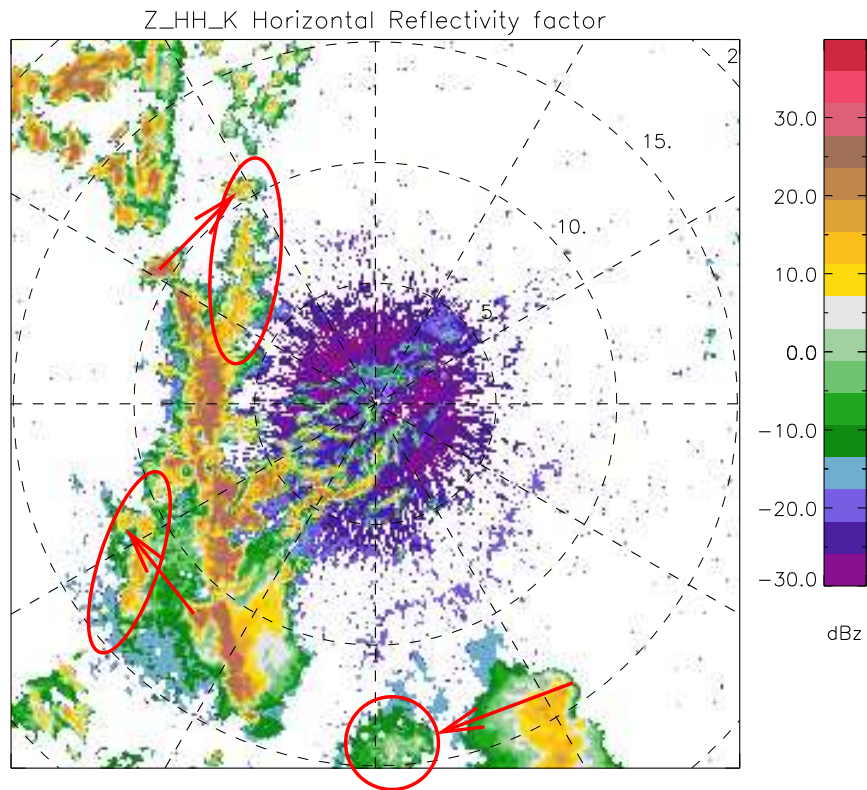
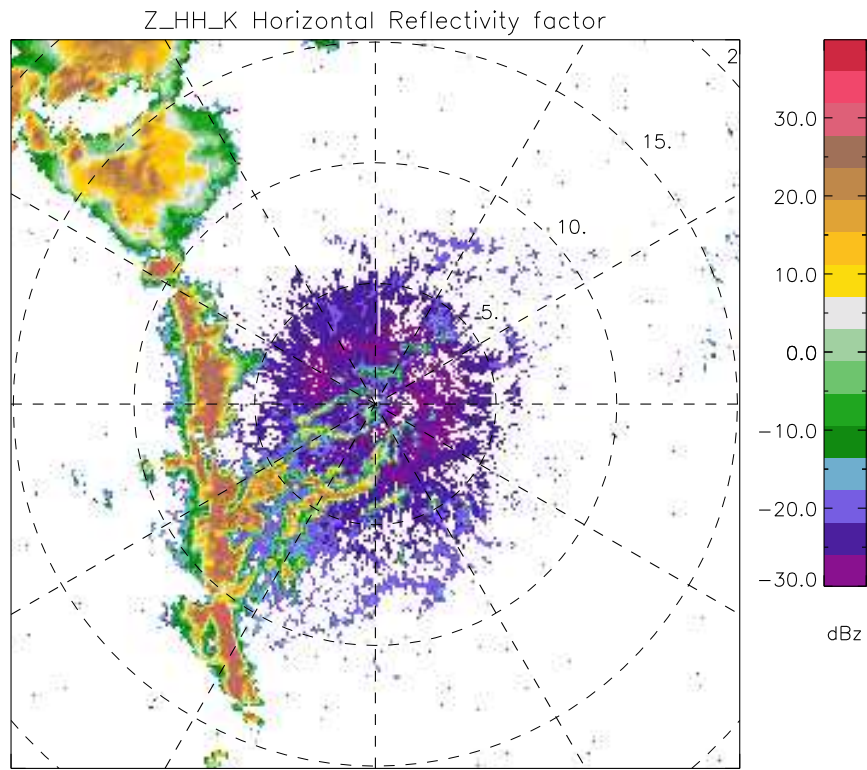
Echoes of features offset in azimuth and attenuated in power (ghost echoes) occurred during the experiment. In contrast to RICO, these appeared to be far more intermittent, sometimes occurring only for part of a scan. The extent of the ghost echo contamination of this data set has not been thoroughly reviewed.

## 4.3 Periods of Useful Data

Based on the summary plots of the engineering log file parameters, it is recommended that the following periods of operation should be used for initial studies.

Table 6: Periods of  $K_a$ -band with a high confidence of reasonable data quality. Time is UTC time.

Date	Start Time	End Time
2006/07/17	21:00	22:20
2006/07/17	22:30	00:00
2006/07/18	16:20	00:00
2006/07/20	17:00	22:00
2006/07/20	23:10	00:00
2006/07/21	16:00	23:30
2006/07/22	16:30	22:00
2006/07/23	17:30	00:00
2006/07/26	15:50	18:10
2006/07/26	19:00	00:00
2006/07/27	16:00	23:50
2006/07/28	15:30	00:00
2006/07/29	16:00	18:00
2006/07/29	19:50	00:30
2006/08/06	16:30	00:00
2006/08/07	16:00	00:20



ncswp\_SPOL\_20060726\_181752.301\_u1\_s1\_1.3\_SUR\_nc

Figure 6: The top image shows a 1.3 degree scan in which the foothills can clearly be seen. This image is not contaminated with ghost echoes. Examples of the ghost echoes in the bottom image have been circled in red and arrows indicate the azimuthal displacement from the real feature to the ghost echo.

# A Engineering Log

2006.07.11

- Lab measurements
- SFD-319 SN: SFD-319/3585/7526
- Center frequency in lab @ 480 Hz, 0.5 us is 34769 MHz
- Delay between tx trigger and RF detected pulse is 550 ns
- TxPh is nominally 1.23 V, TxPv is nominally 1.00 V
- Transmitter power at the output of the transmitter cabinet is +77.2 dBm

2006.07.12

- Lab measurements
- Receiver gain:
  - H-channel: 44.96 dB
  - V-channel: 44.06 dB
- Noise figure:
  - H-channel: 7.0 dB
  - V-channel: 7.8 dB
- Loss from tx port on the receiver cabinet to the H-channel antenna port is 4.1 dBm, loss from tx port on the receiver cabinet to the H-channel antenna port is 4.1 dBm

2006.07.13

- Ka-band installation begins

2006.07.14

- Ka-band installation complete
- RDA configuration to support Ka-band
- Ka-band testing begins

2006.07.15

- Ka-band testing

2006.07.16

- Ka-band testing

2006.07.17

- Ka-band up, dish not aligned

2006.07.18

- Ka-band up

- Ka-band processor restarted at 17:33

2006.07.19

- Ka-band down, GPS disciplining issues
- Dish alignment complete

2006.07.20

- Ka-band up
- Ka-band transmitter tripped breaker at 2210 during vertical pointing scan
- Ka-band back up at 2253

2006.07.21

- Changed log file formatting for TxPh and TxPv to %f1.3
- Ka-band up

2006.07.22

- Ka-band up

2006.07.23

- Log file formatting for TxPh and TxPv changed by mistake to %f3.1
- Changed hard-coded test target gates used to compute test target power in logfile
- Changed V-channel sampling delay (tpdelay2) from 5 (500 ns) to 3 (300 ns) to align H and V channels
- Ka-band up

2006.07.24

- Ka-band transmitter nitrogen leak, Ka-band down

2006.07.25

- Ka-band up

2006.07.26

- Ka-band up
- First ghost echoes noticed

2006.07.27

- Ka-band up

2006.07.28

- Ka-band up

2006.07.29

- Ka-band up

2006.07.30

- Ka-band up
- Large ZDR change at 21:09
- Ghost echoes observed at 23:04

2006.07.31

- Ka-band up
- GO intermittent at 17:04 but became stable
- Ghost echoes at 22:55
- Ghost echoes 23:10:57 when diff\_PN = 3
- Ka-band down between 00:18 and 01:04
- All night operations

2006.08.01

- Changed log file formatting for TxPh and TxPv to %f1.3
- Ka-band down at 15:08
- Ka-band up at 15:36
- Ka-band receiver losing lock on transmitted pulse, Ka-band down at 1915
- th\_vh\_k, zdr, and rhohv\_k changed at 23:24, but back to normal at 23:56

2006.08.02

- Ka-band up

2006.08.03

- V-channel LNA changed (V-channel uncalibrated)
- Ka-band up

2006.08.04

- Changes to processor code to fix ghost echoes at 16:22:
  - fifo.c: d = Pointer(Sampler->pulsenum-1);
  - global.c: OSC3\_limit 1.0e6 -> 0.5e6  
OSC3\_step 10 -> 5
- Ka-band up at 16:38
- zdr\_k and th\_vh\_k not right at 16:50
- Receiver unable to track transmitted pulse at 17:14

- Ka-band down at 17:44

2006.08.05

- Changed tuning screw on 20 MHz oscillator approximately 1/4 turn anti-clockwise to fix 1 PPS disciplining (information from Mitch Randall)
- Measured delay between tx trigger and RF detected pulse at 660 ns
- Ka-band down

2006.08.06

- Increased magnetron HV by 200 V to flatten pulse
- Changed tpdelay from -6 to -7 to compensate for shift in transmitted pulse
- Ka-band up

2006.08.07

- Ka-band up

2006.08.08

- Replaced H-channel LNA and TR limiter; H-channel gain not calibrated
- Transmitter MAG AVG CUR fault at 16:28, turned HV down from 22.6 kV to 22.4 kV

2006.08.09

- Replaced Ka-band LNAs, system not calibrated
- Ka-band down

## References

- [1] D. M. Pozar. *Microwave Engineering*. John Wiley & Sons, Inc., second edition, 1998.
- [2] H. Schrank. Antenna designer's handbook. *IEEE Antennas and Propagation Society Newsletter*, pages 8–9, December 1984.